Nuclear Engineering and Design 241 (2011) 3042–3050

Contents lists available at ScienceDirect

Nuclear Engineering and Design

journal homepage: www.elsevier.com/locate/nucengdes

On-line reconstruction of in-core power distribution by harmonics expansion method

Changhui Wang, Hongchun Wu, Liangzhi Cao*, Ping Yang

School of Nuclear Science and Technology, Xi'an Jiaotong University, Xi'an, Shaanxi 710049, PR China

ARTICLE INFO

Article history:
Received 5 January 2011
Received in revised form 3 May 2011
Accepted 9 May 2011

ABSTRACT

Fixed in-core detectors are most suitable in real-time response to in-core power distributions in pressurized water reactors (PWRs). In this paper, a harmonics expansion method is used to reconstruct the in-core power distribution of a PWR on-line. In this method, the in-core power distribution is expanded by the harmonics of one reference case. The expansion coefficients are calculated using signals provided by fixed in-core detectors. To conserve computing time and improve reconstruction precision, a harmonics data library containing the harmonics of different reference cases is constructed. Upon reconstruction of the in-core power distribution on-line, the two closest reference cases are searched from the harmonics data library to produce expanded harmonics by interpolation. The Unit 1 reactor of DayaBay Nuclear Power Plant (DayaBay NPP) in China is considered for verification. The maximum relative error between the measurement and reconstruction results is less than 5.5%, and the computing time is about 0.53 s for a single reconstruction, indicating that this method is suitable for the on-line monitoring of PWRs.

1. Introduction

In nuclear reactors, the three-dimensional (3D) in-core power distribution continuously and complexly changes due to the movement of control rods, the feedback effects of reactivity, and the burn-up of fuel, among others. Thus, to ensure the safety of reactors, monitoring the in-core power distribution continuously is necessary.

Three types of detectors have been developed to determine in-core power distribution in PWRs: ex-core neutron detectors, movable detectors, and fixed in-core detectors. Ex-core neutron detectors are widely used to provide information of in-core power on the axial direction. However, with the influence of noise, the reliability of measurements from ex-core detectors is low; these detectors poorly give out 3D in-core power distributions. Movable detectors are used in movable detector systems that are implemented once every month to obtain reliable 3D power distributions in PWR cores. However, movable detectors cannot provide real-time information. Fixed in-core detectors provide information of in-core power distribution with higher reliability compared with ex-core detectors. More and more stations, such as Seabrook (Gorski and Cacciapouti, 1996) and Ringhals (Andersson et al., 1996), are using fixed in-core detectors in determining 3D power distributions.

Many kinds of on-line monitoring systems, such as BEACON (Boyd and Miller, 1996) and GNF-ARGOS (Tojo et al., 2008), have been developed to estimate in-core power distributions using fixed in-core detectors. The basic idea behind these systems is calculating 3D power distributions on-line and adapting the calculation results based on detector readings. The detector weighting function plays an important role in the adaptation. However, there are two evident limitations in these systems. First, many experiments have to be performed to verify the reliability of the detector weighting function. Second, the weighting function reaches zero at the region far from the detector (Alejandro et al., 1999), leading to adaptation failure. An alternative means, named harmonics expansion method, is therefore employed in in-core power reconstruction (Li et al., 1997). This alternative means was further studied by Wang and Li (2003) for the on-line monitoring of reactor power distributions, with emphasis on heating reactors with ex-core detectors. However, with the low reliability of ex-core detectors, the relative error between reconstructed and actual values even reaches 15% (Wang, 2001), which is beyond the acceptance criterion (8%) set by the National Nuclear Safety Administration (NSSA).

In this research, fixed in-core detectors are employed to reconstruct in-core power distributions on-line using the harmonics expansion method.

Harmonics, which are eigenfunctions of the neutron diffusion equation, compose a set of complete orthogonal basic functions. Thus, the in-core power distribution for any case can be theoreti-

* Corresponding author at: Department of Nuclear Engineering, Xi'an Jiaotong University, 28 Xianning West Road, Xi'an, Shaanxi 710049, PR China.
Tel.: +86 2982663285; fax: +86 2982667802.
E-mail addresses: caolz@mail.xjtu.edu.cn, caoliangzhi@gmail.com (L. Cao).

0029-5493/$ – see front matter © 2011 Elsevier B.V. All rights reserved.
doi:10.1016/j.nucengdes.2011.05.013

cally expanded by harmonics. The on-line reconstruction of in-core power distributions is conducted in two steps: the in-core power distribution is expanded by the harmonics of a reference case, and then the expansion coefficients are calculated on-line using fixed in-core detector readings. In-core power distribution varies complexly with many factors, such as fuel burn-up, boron concentration, movement of control rods, and xenon density. If the harmonics of a fixed reference case are used to expand in-core power distribution anytime, a big warp is produced. Therefore, a harmonics data library that includes the harmonics of different reference cases should be generated in advance. When the reactor condition changes, the system searches for the two closest reference cases from the data library, and then the corresponding harmonics are produced by interpolation. For this purpose, a code package named core on-line monitoring system (COMS) is developed.

This paper is organized as follows. Section 2 introduces the harmonics calculation method. Section 3 describes the harmonics expansion method and the scheme of harmonics data library generation. In Section 4, taking the Unit 1 reactor of DayaBay NPP as an example, some numerical calculations are performed to verify the accuracy of the harmonics expansion method. Conclusions are given in the last section.

2. Harmonics calculation method

Harmonics calculation is the groundwork of the harmonics expansion method. In the past several years, the power iteration method and subspace techniques, such as Krylov subspace method for calculating the harmonics of the neutron diffusion equation, have been proposed and investigated by several researchers, including Li (1994) and Warsa et al. (2004). Compared with the power iteration method, the Krylov subspace method has a higher calculation speed in solving eigenvalue problems (Zinzani et al., 2008). Thus, this method is used to calculate harmonics in this paper.

The Krylov subspace method is considered efficient in solving large matrix eigenproblems. Fortunately, the neutron diffusion equation is an eigenproblem that can be given by the operator in the following equation:

$$M\Phi = \frac{1}{k}F\Phi \tag{1}$$

where M and F are neutron loss and production operators, respectively. By kM^{-1}, Eq. (1) can be transformed into the following standard-form eigenproblem:

$$A\Phi = k\Phi \tag{2}$$

where $A = M^{-1}F$. The dimension of operator A is decided by the number of spatial mesh and energy group. For commercial PWRs, operator A is a large matrix.

Theoretically, Eq. (2) has serial eigenpairs (Φ_i,k_i). In this paper, the eigenvectors $\{\Phi_1,\Phi_2,\ldots,\Phi_N\}$ with $k_1 > k_2 > \cdots > k_N$ are defined as the harmonics of the neutron diffusion equation. The Φ_i is defined as the ith order of the harmonics. The Krylov subspace method is employed to calculate the harmonics. The main idea behind this method is constructing the approximate eigenpairs of matrix A from a subspace K_m. The process can be described as follows:

(1) Choose an initial value of m, and calculate the Krylov subspace K_m. The Krylov subspace is defined as $K_m = \{r_0, Ar_0, \cdots, A^m r_0\}$ for the eigenproblem $A\Phi = k\Phi$, where r_0 is an initial vector; $r_0 \in R^n$, $A \in R^{n\times n}$, and $\Phi \in R^n$.
(2) An orthonormal basis V_m is drawn from the space K_m according to the Arnoldi algorithm (see Arnoldi algorithm). At the same time, an upper Hessenberg matrix H_m is obtained. The forms of V_m and H_m are as follows:

$$V_m = \{v_1,\ v_2,\ \ldots,\ v_m\} (V_m \in R^{n\times m})$$

$$H_m = \begin{bmatrix} h_{1,1} & h_{1,2} & \cdots & h_{1,m-1} & h_{1,m} \\ h_{2,1} & h_{2,2} & \cdots & h_{2,m-1} & h_{2,m} \\ 0 & h_{3,2} & \ddots & & \vdots \\ \vdots & \ddots & \ddots & \ddots & \vdots \\ 0 & \cdots & 0 & h_{m,m-1} & h_{m,m} \end{bmatrix} (H_m \in R^{m\times m})$$

According to the Arnoldi algorithm, the orthonormal basis V_m and the matrix H_m are related as follows:

$$AV_m = V_m H_m + h_{m+1,m} v_{m+1} e_m^T \tag{3}$$

where $e_m^T = \underbrace{(0, 0, \cdots 1)}_{m}$ and $V_m^H v_{m+1} = 0$. Here, V_m^H is a generalized inverse matrix of V_m.

By multiplying both sides of Eq. (3) by V_m^H, we obtain

$$H_m = V_m^H A V_m \tag{4}$$

(3) The solutions of Eq. (2) are expanded by the orthonormal basis H_m.

$$\Phi = V_m y_m \tag{5}$$

where y_m is a vector of the expansion coefficients.

By substituting Eq. (5) into Eq. (2), we obtain

$$H_m y_m = k y_m \tag{6}$$

(4) If m is far less than n, it becomes much easier to calculate the eigenpairs of matrix H_m than matrix A. The eigenpairs (y_m,k) of matrix H_m can be obtained conveniently by QR factorization. Subsequently, the eigenpairs (Φ,k) of matrix A can be obtained according to Eq. (5).
(5) If the eigenpairs (k,Φ) do not satisfy the requirement of convergence, we add one to m and steps (1)–(4) are repeated.

For a commercial PWR, operator A is a large matrix whose dimension is approximately 3.32×10^6. Theoretically, the harmonics of matrix A can be calculated using the Krylov subspace method as described above. However, given the oversized matrix, parameter m must be large enough. Hence, the costs of memory storage and CPU time are increased. To avoid this drawback, a method named implicit restarted Arnoldi method (IRAM) has been proposed. IRAM restarts the Krylov subspace method process with a new starting vector r_0, which is usually updated to enhance components in the directions of the desired eigenvectors and to depress components in other directions. In this paper, the harmonics of the neutron diffusion equation are calculated using IRAM.

A FORTRAN code named CITK is developed in this study for harmonics calculation.

Arnoldi algorithm
For a Krylov subspace $K_m = \{r_0,\ Ar_0,\ \ldots,\ A^m r_0\}$,
Set $v_1 = \frac{r_0}{\|r_0\|_2}$;
For $i = 1,\ 2,\ \ldots,\ m$
$v_i = \frac{Av_{i-1} - \sum_{k=1}^{i-1} \langle Av_{i-1}, v_k\rangle v_k}{\|Av_{i-1} - \sum_{k=1}^{i-1} \langle Av_{i-1}, v_k\rangle v_k\|_2}$
For $j = 1,\ 2,\ \ldots,\ i-1$
$h_{j,i-1} = \left\langle Av_{i-1}, v_j \right\rangle$
End
$h_{i,i-1} = \|Av_{i-1} - \sum_{k=1}^{i-1} \left\langle Av_{i-1}, v_k \right\rangle v_k\|_2$
If $h_{i,i-1} = 0$, break
End

3. Harmonics expansion method

As previously mentioned, harmonics refer to a serial of eigenfunctions of the neutron diffusion equation. Due to its completeness and orthogonality, harmonics compose a set of complete orthogonal basic functions. Therefore, in-core power distribution for any case can be expanded by the harmonics of a reference case.

3.1. Harmonics expansion method

We expand the power distribution of a PWR with the harmonics of a reference case:

$$P(r) = \sum_{i=1}^{N} a_i \Phi_i(r) \tag{7}$$

where $P(r)$ is the power distribution, N is the total order of harmonics, and r is a spatial variable.

To reconstruct the in-core power distribution on-line, some real-time information is necessary. Various information on $P(r)$ can be obtained on-line using fixed in-core detectors. In a PWR, the fixed in-core detectors are located in the instrumentation tube of the fuel assemblies and the readings of the detectors are proportional to the local power. Considering that a total of N_D detectors are installed in the reactor and their locations are $r_k (k = 1, 2, \ldots, N_D)$, then the detector readings $R(r_k)$ can be written as follows:

$$R(r_k) \propto P(r_k) = \sum_{i=1}^{N} a_i \Phi_i(r_k) \tag{8}$$

Subsequently, the following equations can be obtained from the N_D detectors:

$$\begin{cases} R(r_1) \propto \sum_{i=1}^{N} a_i \Phi_i(r_1) \\ R(r_2) \propto \sum_{i=1}^{N} a_i \Phi_i(r_2) \\ \vdots \\ R(r_{N_D}) \propto \sum_{i=1}^{N} a_i \Phi_i(r_{N_D}) \end{cases} \tag{9}$$

The expansion coefficients a_i can be calculated using the least square method from Eq. (9) if $N_D \geq N$, and the in-core power distribution $P(r)$ can be reconstructed conveniently according to Eq. (7).

The accuracy of the reconstruction is related to the selection of the reference case. The closer the reference case is to the real status, the higher is the reconstruction accuracy. It is because that the corresponding harmonics of closer reference case can more reflect the feature of the real reactor condition. To increase reconstruction accuracy, one must renew the reference case and recalculate the harmonics when the reactor condition changes. However, this is time consuming, which results in the infeasibility of on-line monitoring the reactor. Fortunately, it is proved by numerical results that the relativity is not strong. Choosing some reference cases can meet the accuracy requirements. Therefore, a harmonics data library, which contains a large amount of harmonics from different reference cases, should be generated in advance. In Section 3.2, the method of harmonics data library generation is introduced in detail.

The on-line monitoring steps are described as follows:

- An archiving server collects information on the PWR, including information on fuel burn-up, boron concentration, control rod position, and power level, from the plant computer network.
- The collected information is then used to search for the two closest reference cases from the harmonics data library, and the expanded harmonics are obtained by interpolation.
- From the plant computer network, the fixed in-core detector readings are collected to calculate expansion coefficients, and the in-core power distribution is reconstructed using these values.
- Lastly, the reconstruction results are displayed on screen.

The code package COMS is developed to implement the foregoing steps. Its program flowchart is shown in Fig. 1.

Table 1
Corresponding relationship between power level and control rods (Burn-up is 2.0 GWd/tU).

Relative power	Position in withdrawn steps			
	G1	G2	N1	N2
1.0	225	225	225	225
0.92	144	225	225	225
0.84	90	215	225	225
0.74	54	179	225	225
0.54	5	128	225	225
0.42	5	80	215	225
0.20	5	39	174	225
0.04	5	13	148	225
0.0	5	5	138	225

3.2. Harmonics data library

In preparation for the on-line reconstruction of in-core power distributions by COMS and to promote reconstruction accuracy, the harmonics data library is pre-generated.

The harmonics data library is a collection of the harmonics of different reference cases. It contains information on reference cases and the corresponding harmonics Φ_n^m ($m = 1 \ldots M$, $n = 1 \ldots N$), where M is the total number of reference cases and N is the total harmonics orders for each reference case.

To raise reconstruction accuracy, reference cases should contain conditions of different periods in an operating cycle. Hence, the process by which reference cases are determined is important in harmonics data library generation.

3.2.1. Determining the reference case

Reactor conditions are influenced by several important factors, such as fuel burn-up, boron concentration, control rod positions, power level, burnable poison density, and xenon and samarium density.

However, in the practice of nuclear power plant, for example in Daya Bay NPP, reactor's power level is regulated through moving the power compensation rods which named G1, G2, N1 and N2, respectively. As a result, power level of the reactor has a one-to-one correspondence with position of power compensation rods. Actually, the correspondence provided by Daya Bay NPP is related to burn-up. For example, the relationship between the power level and the control rod position at 2.0 GWd/tU burnup of Daya Bay NPP is shown in Table 1. In a burn-up section, it is assumed that the relationship is constant. So the influence of power level and control rod positions can be seen as identical in a burn-up section.

Under normal operating conditions, xenon and samarium reach their equilibrium density. Hence, as shown in Eq. (10), harmonics can be regarded as a function of fuel burn-up, boron concentration, control rod positions, and burnable poison density.

$$\Phi_n^m = f(Bu,\ Cb,\ Rod,\ Bp) \tag{10}$$

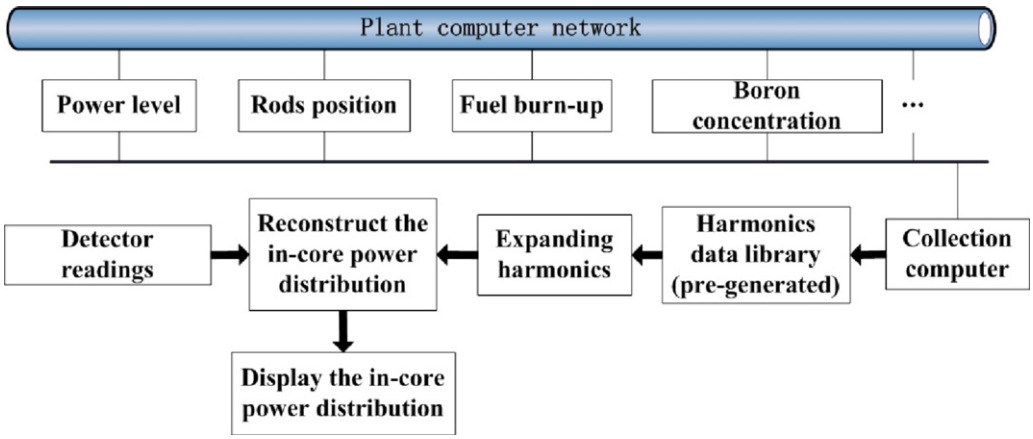

Fig. 1. Flowchart of COMS.

where *Bu*, *Cb*, *Rod*, *Bp* represent fuel burn-up, boron concentration, control rod positions, and burnable poison density, respectively.

To simplify Eq. (10), the effects of these factors can be separated into global and local effects. The global effects are mainly caused by fuel burn-up, boron concentration changes, and exposure to burnable poison, whereas the local effects are caused by control rod movement and fuel burn-up. The harmonics function Φ_n^m can then be regarded as a superposition of these two effects. Eq. (10) can then be written as

$$\Phi_n^m = f_{1,n}^m(Bu,\ Cb,\ Bp) + f_{2,n}^m(Bu,\ Rod) \tag{11}$$

where $f_{1,n}^m$ represents the global effects and $f_{2,n}^m$ stands for the local effects.

After the separation, the global and local effects are considered independently to determine the reference case.

3.2.1.1. Global effects. During an operating cycle, fuel composition constantly varies. Boron concentration and burnable poison density are changed to recompense for the decrease in fissile isotope in the fuel. The variation disciplinarian of fuel composition can be obtained by fuel management calculation.

A fuel management code package named SIMME, developed by Xi'an Jiaotong University, is used successfully in fuel management calculation for many reactors. It is also used in this study to simulate the fuel burn-up process. The nonlinear semi-analytic nodal method (Liao, 2002) is used for neutronics calculation in SIMME, whereas thermal-hydraulic calculation is based on the single channel model.

The reference cases for the global effects are simulated by SIMME. In the simulation, the burn-up step is 0.2 GWd/tU, and all control rods are withdrawn. The harmonics for each reference case are calculated using the CITK code. All of these harmonics construct the global effects as shown in the following equation:

$$f_{1,n} = [\Phi_n^{Bu_1},\ \Phi_n^{Bu_2},\ \ldots,\ \Phi_n^{Bu_L}] \tag{12}$$

where Bu_l is the burn-up step and L is the total number of Bu_l.

3.2.1.2. Local effects. The rule of control rod movements is important for the local effects. For a PWR, there is a fixed procedure for the movement of control rods. For example, in the DayaBay NPP Unit 1 reactor, there are five groups of control rods in the core, named R, G1, G2, N1, and N2. Groups G1, G2, N1, and N2 move according to the procedure shown in Fig. 2, whereas group R moves in an adjustment region (a total of 24 steps). The possible positions of the control rods can be easily determined according to Fig. 2.

As shown in Eq. (11), the local effects are related to both fuel burn-up and control rod positions. To separate the two factors, the burn-up is divided into some sections. In each section, the local effects can be considered as independent of the burn-up. The space of adjacent sections in this study is 1.2 GWd/tU. In each burn-up section, the conditions with different control rod positions are simulated by SIMME, and they are selected as reference cases for the local effects. The harmonics of these reference cases are calculated using CITK code.

In each burn-up section, the difference in harmonics between the rods insert and all rods out (ARO) conditions, which are defined in Eq. (13), indicate the influence of control rods.

$$\delta\Phi_n = \Phi_n^r - \Phi_n^0 \tag{13}$$

where δ signifies the difference, Φ_n^r is the harmonics with control rods located in r, and Φ_n^0 represents the harmonics with ARO.

All of the differences construct the local effects with the following form:

$$f_{2,n} = \begin{bmatrix} \delta\Phi_n^{r_1,Bu_1} & \delta\Phi_n^{r_2,Bu_1} & \ldots & \delta\Phi_n^{r_J,Bu_1} \\ \delta\Phi_n^{r_1,Bu_2} & \delta\Phi_n^{r_2,Bu_2} & \ldots & \delta\Phi_n^{r_J,Bu_2} \\ & \vdots & & \\ \delta\Phi_n^{r_1,Bu_K} & \delta\Phi_n^{r_2,Bu_K} & \ldots & \delta\Phi_n^{r_J,Bu_K} \end{bmatrix} \tag{14}$$

where $r_j (j = 1, 2, \ldots, J)$ are the different control rod positions, J is the total number of r_j, $Bu_k (k = 1, 2, \ldots, K)$ are the burn-up sections, and K is the total number of Bu_k.

3.2.2. Generating the harmonics data library

According to Eq. (11), the harmonics data library is separated into two parts, global effects and local effects, as follows:

$$\begin{cases} f_{1,n} \\ f_{2,n} \end{cases} \quad n = 1,\ 2,\ \ldots,\ N \tag{15}$$

where N is the total order of harmonics for each reference case.

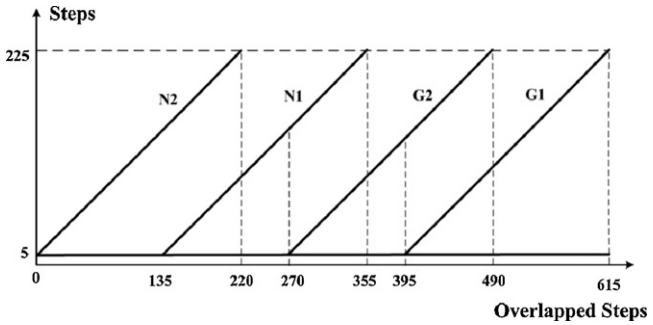

Fig. 2. Movement order of G1, G2, N1, and N2.

Table 2
Selection of basic functions.

Conditions of basic functions			Selected orders
Burn-up (GWd/tU)	Rod positions		
	R (Steps)	G1, G2, N1, N2 (Overlapped steps)	
0.16	225[a]	615[b]	First 20th
3.2	225	615	First 20th
8.0	225	615	First 20th
14.0	225	615	First 20th
18.4	225	615	First 20th
10.0	225	68	First 10th
10.0	225	178	First 10th
10.0	225	245	First 10th
10.0	225	313	First 10th
10.0	225	375	First 10th
10.0	225	443	First 10th
10.0	225	553	First 10th
10.0	208	615	First 10th

[a] Rod clusters *R* are out at 225 steps.
[b] Rod clusters G1, G2, N1, and N2 are all out at 615 overlapped steps.

Considering the DayaBay NPP reactor as an example, J in Eq. (12) is 108, K in Eq. (14) is set at 129, and J in Eq. (14) is 18. If we set N in Eq. (15) at 10, then the total number of elements in the data library, including harmonics and differences in harmonics as defined by Eq. (13), is 24,300. Considering that each element requires a storage space of 4.76 MB, a total of 115,668 MB is required to store all these elements directly in the library. This is impractical.

To reduce the storage requirement, the elements in the data library are expanded by a group of basic functions. The basic functions must then be capable of expanding both global effects and local effects. In this study, the basic functions are selected as the harmonics of some cases with different burn-up and control rod positions, and with the form $[\Psi_1,\Psi_2,\ldots,\Psi_I]$. The selection of the basic functions is shown in Table 2.

The global effects $f_{1,n}$ and local effects $f_{2,n}$ are expanded using the basic functions as follows:

$$f_{1,n} = A_{1,n}[\Psi_1,\ \Psi_2,\ \ldots,\ \Psi_I]^T \tag{16}$$

$$f_{2,n} = A_{2,n}[\Psi_1,\ \Psi_2,\ \ldots,\ \Psi_I]^T \tag{17}$$

where $A_{1,n}$ and $A_{2,n}$ are the coefficient matrices, and $A_{1,n} \in R^{L\times I}$ and $A_{1,n} \in R^{(jk)\times I}$. Information on global effects and local effects can be stored as the coefficient matrices $A_{1,n}$ and $A_{2,n}$.

The ultimate structure of the harmonics data library is shown in Table 3.

4. Numerical results

4.1. Accuracy of harmonics calculation

In this study, the code CITK is developed for harmonics calculation. In this code, the space is discretized by the finite difference method and harmonics are calculated using the Krylov subspace method. The 3D IAEA benchmark problem is calculated to validate the accuracy of harmonics calculation.

Table 3
Structure of harmonics data library.

Stored information	Storage (MB)
Information of reference cases	0.093
Basic functions: $[\Psi_1,\ \Psi_2,\ \ldots,\ \Psi_I]$	856.8
Coefficient matrices: $A_{1,n}$ and $A_{2,n}$	9.56

Table 4
Eigenvalues of the IAEA benchmark.

Orders	Reference k_i*	k_i	$\frac{\|\|\varepsilon_i\|\|_2}{\|\|M\Phi_i\|\|_2}$
1	1.02903	1.028902	0.00157
2	–	1.014865	0.00162
3	–	1.002229	0.00200
4	–	0.994688	0.00169
5	–	0.990508	0.00195
6	–	0.990262	0.00213
7	–	0.977698	0.00202

* Reference k_i is from Bandini (1990).

Harmonics, which are the eigenvectors of neutron diffusion equation, satisfy the equation $M\Phi_i = (1/k_i)F\Phi_i$. Here, a residual vector is defined as follows:

$$\varepsilon_i = M\Phi_i - \frac{1}{k_i}F\Phi_i \tag{18}$$

In theory, the residual vector falls to zero if the harmonics calculation is correct. However, in the numerical calculation, the residual vector becomes infinitesimal. Here, we use $(||\varepsilon_i||_2/||M\Phi_i||_2)$ to represent the convergence of the residual vector. The results are presented in Table 4.

Based on Table 4, the relative error of k_1 compared with the reference result is −0.012%. The 2-norm of ε_i is lower than that of $M\Phi_i$ by three orders of magnitude. This indicates that the residual vector converges to nearly zero. The results prove that the harmonics calculation of CITK is correct.

The IAEA benchmark is a two-energy-group neutron diffusion problem. The first group is the fast group, and the second group is the thermal group. Correspondingly, the harmonics is divided into two groups, fast harmonics and thermal harmonics. The radial plots of the thermal harmonics for the first four orders of the IAEA benchmark obtained from CITK are shown in Fig. 3.

4.2. On-line reconstruction of power distribution for the DayaBay NPP reactor

The code package COMS is developed to reconstruct in-core power distribution in this research. To verify the accuracy of COMS results, a criterion should be initially introduced. An acceptance criterion is issued by NNSA for reactor monitoring. The maximum RE must be less than 5% in assemblies with relative power (Pr) of more than 0.9, and the maximum RE must be less than 8% in assemblies with Pr of less than 0.9.

In this section, numerical experiments are performed. A commercial PWR is employed, and some of the results are exhibited.

4.2.1. Problem description

To validate the accuracy of power reconstruction using COMS, the Unit 1 reactor of DayaBay NPP is tested. The reactor core consists of 157 assemblies. Each assembly incorporates 264 fuel rods, 24 guide thimbles, and one instrumentation tube. We compare reconstruction results from COMS and measurements from DayaBay NPP. The fixed in-core detectors are located in the same radial core locations as the movable detector system "◯" as shown in Fig. 4. In each tube, five detectors fall in the mid regions between the assembly grids as presented in Fig. 5.

4.2.2. Comparison of measurements

Sixteen measurements of different burn-up cases of DayaBay NPP are provided. The measurements include measured power distributions and detector readings from movable in-core detectors. It should be mentioned that the fixed in-core detectors have not been located in the DayaBay NPP reactor. However, at the same location,

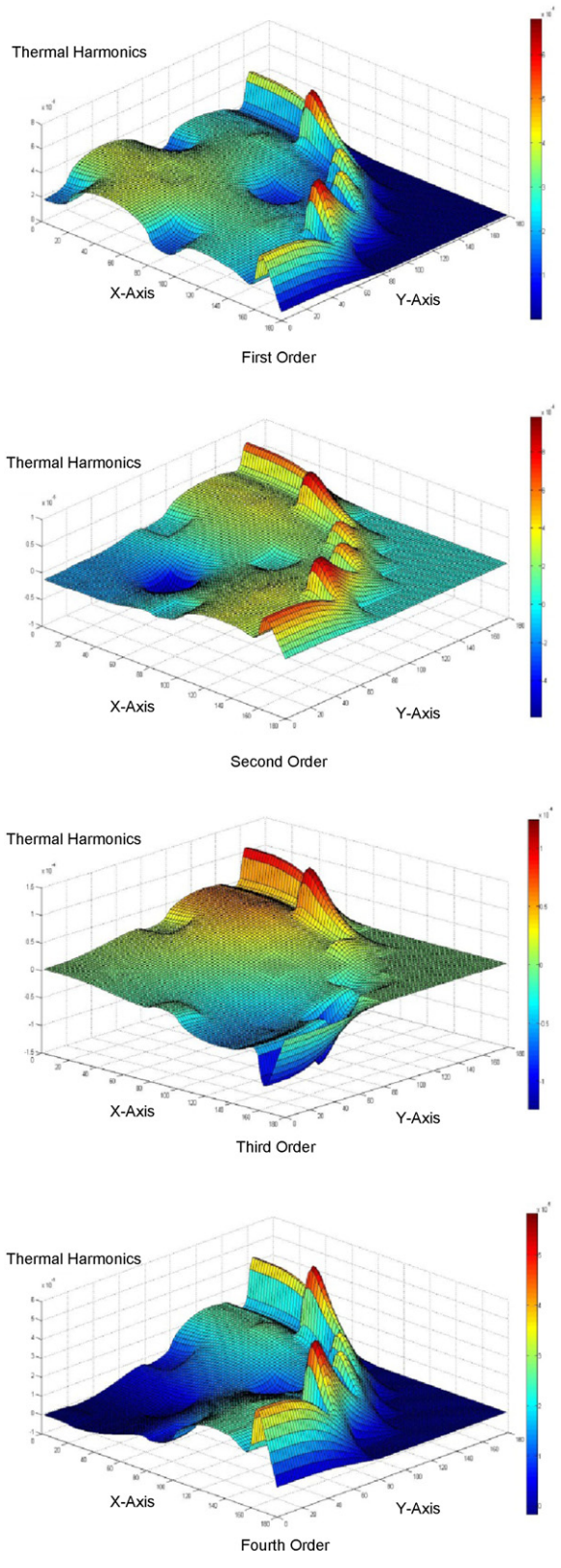

Fig. 3. Radial plots of thermal harmonics.

the readings of the fixed in-core detectors can be regarded as the same as that of the movable detectors.

The in-core power distribution with different burn-up is reconstructed by COMS using fixed in-core detector readings. Fig. 6 shows the relative errors between the reconstruction results and

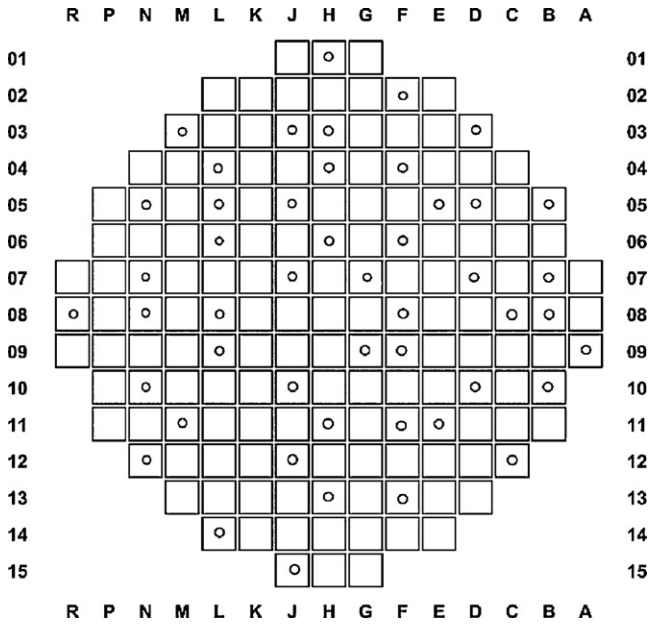

Fig. 4. Locations of the fixed in-core detectors.

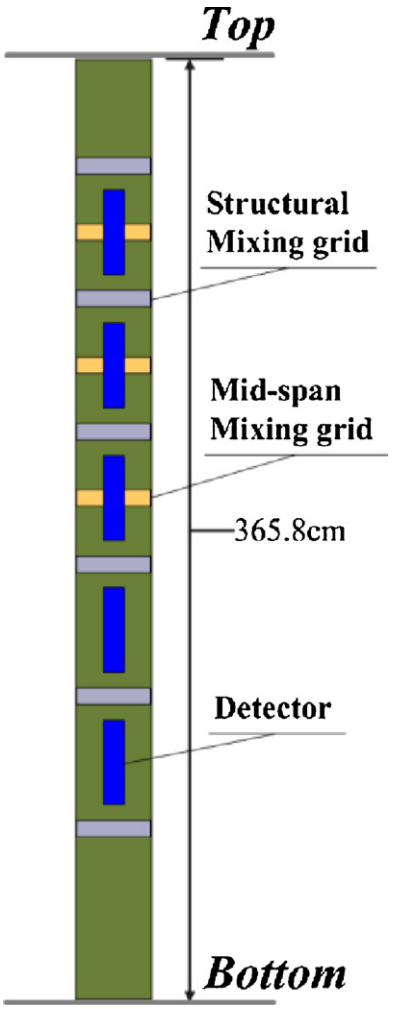

Fig. 5. Detector arrangement in the assembly.

	R	P	N	M	L	K	J	H	G	F	E	D	C	B	A
01							-2.2*	-2.5	-0.6						
02					-2.6	-1.3	-0.6	1.0	0.0	-0.9	-1.7				
03				2.1	-0.4	0.3	1.0	2.0	2.4	1.5	0.5	2.7			
04			1.9	0.8	1.3	0.4	0.8	1.8	1.9	1.4	1.8	0.9	1.6		
05		-3.0	-0.6	1.1	0.9	-0.5	-0.4	0.9	0.3	0.0	1.1	0.8	-1.2	-3.7	
06		-1.7	-0.1	0.1	-0.6	-1.6	-0.3	0.6	0.1	-1.5	-0.8	-0.6	-0.9	-2.6	
07	-2.8	-1.2	-0.5	0.4	-0.6	-0.4	-0.1	0.2	0.1	-0.5	-1.1	-0.4	-0.6	-2.4	-4.1
08	-4.3	-1.2	0.4	0.5	-0.1	0.1	-0.1	-1.2	0.2	0.2	0.1	0.6	0.5	-1.1	-4.2
09	-3.5	-1.9	-0.2	-0.2	-1.0	-0.7	-0.3	-0.0	-0.0	-0.3	-0.3	0.8	1.1	-0.5	-2.0
10		-2.2	-0.6	-0.4	-0.9	-1.7	-0.4	0.3	-0.3	-1.5	-0.4	0.5	0.5	-1.1	
11		-3.4	-1.0	0.9	0.9	-0.4	-0.2	0.5	-0.5	-0.5	1.1	1.4	-0.2	-2.5	
12			1.7	0.8	1.5	0.9	1.2	1.3	0.6	0.3	1.3	1.0	2.2		
13				2.3	0.0	0.8	1.6	1.5	0.7	0.2	-0.4	2.1			
14					-2.3	-0.8	0.0	-0.1	-0.9	-1.5	-2.8				
15							-1.5	-3.2	-2.5						

*(Reconstruction – Measurement)/Measurement*100.

Assemblies with Pr more than 0.9.

Assemblies with Pr less than 0.9.

Fig. 6. Relative error distribution (Burn-up is 3.703 GWd/tU).

the measurements. The axial power distribution is presented in Fig. 7. In Fig. 8, the maximum relative errors (RE) between the reconstruction and the measurement results with different burn-up are presented. The location of the maximum RE is shown as "A08" in Fig. 8, and the root mean square (RMS) errors of the diffusion calculation and reconstruction results are also shown in the same figure.

Fig. 6 shows that COMS provides credible results. For the presented case, the RE between the measurement and reconstruction results are less than 4.3% in all assemblies. In the assemblies with Pr of more than 0.9, the maximum RE is 2.4%, which is under the acceptance criterion. For assemblies with Pr of less than 0.9, the RE increase because of the low power level in these assemblies. However, the maximum RE (4.3%) in these assemblies is also under the acceptance criterion.

Fig. 7 shows the axial power distribution of the reconstruction results, which agrees well with the measurement results.

For most cases, RMS errors of the reconstruction results are lower than those of the diffusion calculation (Fig. 8). Compared with the diffusion results, the RMS reconstruction errors are more stable, and are kept at less than 2.3%. This proves that the harmonics expansion method is applicable for the entire operating cycle. Fig. 8 also shows that the maximum relative errors are less than 5.5%, and all of the errors appear near the boundary of the core.

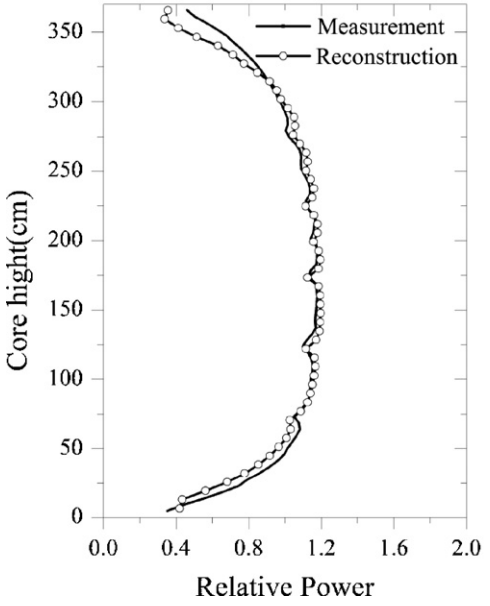

Fig. 7. Axial power distribution (Burn-up is 3.703 GWd/tU).

4.2.3. Reconstruction with different control rod positions

For the Dayabay NPP reactor, the control rods G1, G2, N1, and N2 are withdrawn when the measurements are conducted. Thus,

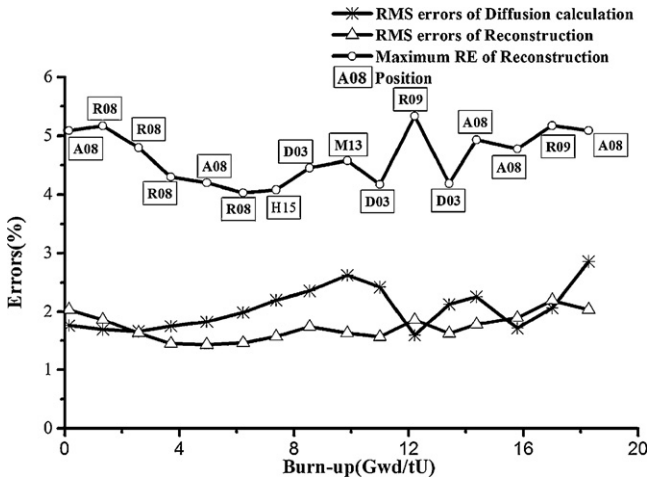

Fig. 8. Relative errors with different burn-up.

another numerical experiment is performed to verify the adaptability of COMS considering different rod positions.

For an arbitrary burn-up (here, 11 GWd/tU is chosen as an example), the rods G1, G2, N1, and N2 are moved from the bottom to the top according to the overlapping steps shown in Fig. 2. In this case, the in-core power distribution and detector readings are supposed as numerical results from a diffusion calculation. The results as reconstructed by COMS are shown in Fig. 9.

RMS errors, considering different rod positions, are mostly less than 1.0% (Fig. 8), suggesting that COMS adapts well to power distribution reconstruction with different rod positions.

4.2.4. Reconstruction with low power conditions

An experiment at low power conditions is done to present the accuracy of harmonics expansion method. In this experiment, the reactor operates from startup to the state at burn-up 1.5 GWd/tU with full power. Then, reactor power level goes down to 50% and 30%, respectively, and operates from 1.5 GWd/tU to 2.5 GWd/tU with steady power. The process described above is simulated by diffusion calculation. The results reconstructed by COMS are shown in Fig. 10.

The numerical results show that the RMS errors are lower than 2.0%. It proves the adaptability of COMS with low power conditions.

4.2.5. Response time

High calculation speed is a basic requirement for on-line monitoring systems. Given the existing on-line monitoring system BEACON for example, the response time is 3–5 min (Fujituka et al., 1996), which is considered quick enough to meet the requirement of reactor on-line monitoring. Therefore, the response time of COMS should be no longer than 5 min. The CPU time (2.66 GHz CPU with a 2.00 GB memory) utilized by COMS, including the time used for harmonics data library reading, detector reading input, expansion coefficient computation, and result file recording, is 0.53 s. Compared with BEACON, COMS is much faster, enabling it to meet the requirement of on-line monitoring.

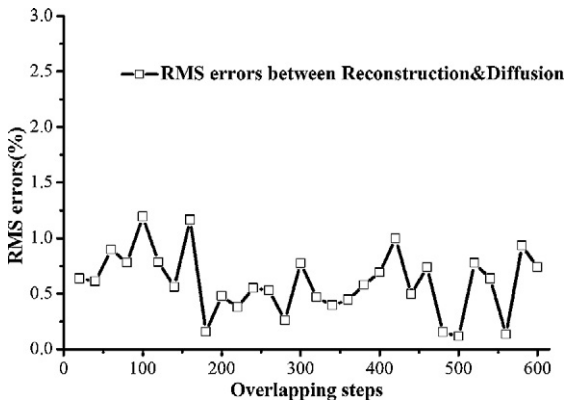

Fig. 9. RMS errors considering different control rod positions.

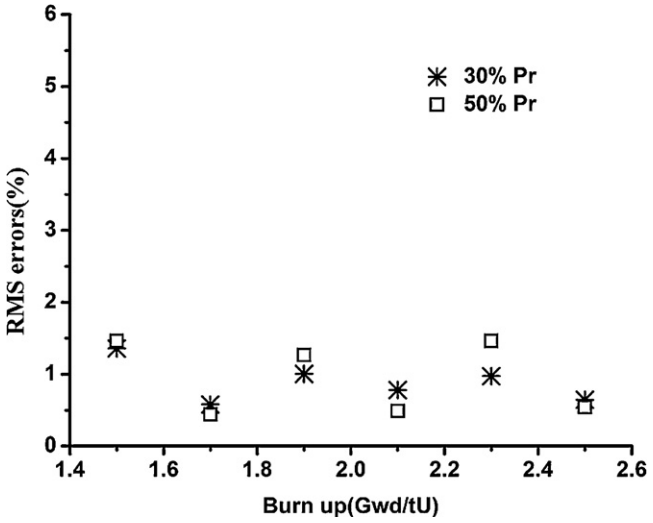

Fig. 10. RMS errors with low power conditions.

4.2.6. Influence of detector failure

During an operating cycle, it is unavoidable that some fixed in-core detectors lose their efficacy. A sensibility analysis is then necessary to verify the influence of detector failure in the harmonics expansion method. An extreme case in which the detectors gradually lose their efficacy from the center to the edge is assumed in the

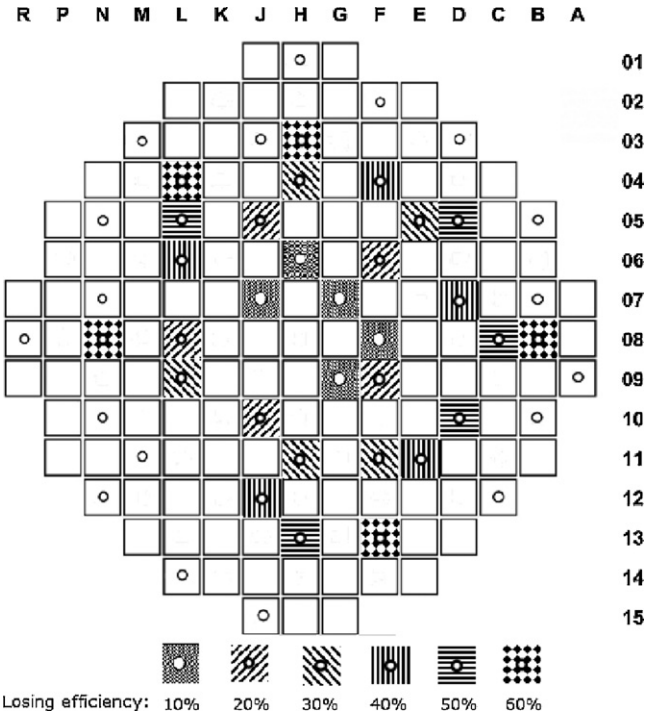

Fig. 11. Assumed losing efficiency order of the detectors.

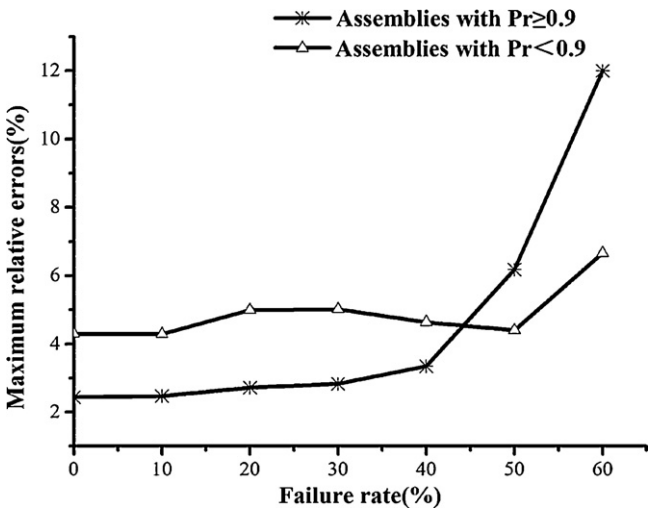

Fig. 12. Influence of failure rate.

following sensibility analysis, as shown in Fig. 11. Detectors in the shadows fall into failure from 10% to 60%. The in-core power distribution with burn-up of 3.703 GWd/tU is reconstructed by COMS. Fig. 12 shows the influence of detector failure rate in the assumed case.

As assumed, the detectors gradually fall into failure from the center to the edge. This causes an evident increase in the RE of the central assemblies. When the failure rate reaches 40%, the maximum RE is 3.35% in the assemblies with $Pr \geq 0.9$, and the maximum RE is 4.64% in the assemblies with $Pr < 0.9$, both of which are under the acceptance criterion. When the failure rate reaches 50%, the maximum RE in the assemblies with $Pr \geq 0.9$ increases to 6.18%, which is over the acceptance criterion.

From the results, it is inferred that COMS works well even at a failure rate of less than 40% in the worst case scenario.

5. Conclusions and future work

This paper presents the concept of using the harmonics expansion method to reconstruct reactor power distributions on-line. A harmonics data library is pre-generated off-line. A code named COMS is developed.

The Unit 1 reactor of Dayabay NPP is taken as an example to verify the accuracy of this method. The following conclusions are drawn from the study:

- Reconstruction results show that RMS errors are less than 2.3% during the operating cycle. The maximum relative errors, which appear at the edge, are less than 5.5%. The in-core power distribution reconstructed by COMS is credible with relative errors in all assemblies under the acceptance criterion set by NNSA.
- The harmonics expansion method is not sensitive to detector failures. Meanwhile, the reconstruction results can meet the requirement of the acceptance criterion, even at a detector failure rate of 40%. This proves that the harmonics expansion method is capable of dealing with detector failures.
- For on-line reactor monitoring, a high calculation speed is necessary. COMS, running on an ordinary personal computer, has a response time of about 0.53 s, which is satisfactory enough for real-time monitoring.

In this paper, harmonics expansion method is employed in on-line reconstruction the power distribution of reactor with steady state. The results show that the method is capable for on-line monitoring the reactor with steady state. Meanwhile, the capability of monitoring the transient conditions of a reactor is another important part for an on-line monitoring system. This issue will be researched in future work.

Acknowledgements

This research was carried out under the financial support of the National Science Foundation of China (Approved numbers 10875094 and 10976021) and the National High Technology Research and Development Program ('863' Program) of China (Approved number 2009AA050705) and the National Magnetic confinement Fusion Science Program (No. 2010GB111007).

References

Alejandro, N., Lorne, C., Nilsson, A., Greiner, D., 1999. Core monitoring based on advanced nodal methods: Experience and plans for further improvements and development. In: Core Monitoring for Commercial Reactors: Improvements in Systems and Methods, Stockholm, Sweden.

Andersson, T., Berg, Ø., Romslo, K., 1996. Ringhals-2 core monitoring experience. In: In-Core Instrumentation and Reactor Core Assessment, Mito-shi, Japan.

Bandini, R., 1990. A three-dimensional transient neutronics routine for the TRAC-PF1 reactor thermal hydraulic computer code. Pennsylvania State University, Pennsylvania.

Boyd, A., Miller, W., 1996. The BEACON on-line core monitoring system: functional upgrades and applications. In: In-Core Instrumentation and Reactor Core Assessment, Mito-shi, Japan.

Fujituka, N., Tanouchi, H., Imamura, I., Mizobuchi, D., Kanagawa, T., Masuda, M., 1996. Experience and evaluation of advanced on-line core monitoring system BEACON at Ikata Site. In: In-Core Instrumentation and Reactor Core Assessment, Mito-shi, Japan.

Gorski, P., Cacciapouti, J., 1996. Experience with fixed in-core detectors at Seabrook Station. In: In-Core Instrumentation and Reactor Core Assessment, Mito-shi, Japan.

Li, F., 1994. Harmonics Synthesis Method for Core Flux Distribution Reconstruction and its Application to Diagnosis. National Tsing Hua University, Beijing.

Li, F., Luo, P., Hu, M., 1997. Harmonics synthesis method for core flux distribution reconstruction. J. Prog. Nucl. Energy 31 (4), 369–372.

Liao, K., 2002. Study on Numerical Method for Three Dimensional Nodal Space-Time Neutron Kinetic Equations and Coupled Neutronic/Thermal-Hydraulic Core Transient Analysis. Xi'an Jiaotong University, Xi'an.

Tojo, M., Naka, T., Iwamoto, T., 2008. Application of the new core monitoring system, 'GNF-ARGOS', to the start-up tracking calculation of ABWR. In: International Conference on the Physics of Reactors , Interlaken, Switzerland.

Wang, Q., 2001. Study of On-line Monitoring the Power Distribution in a Reactor Core by Using Ex-core Ion-chambers. National Tsing Hua University, Beijing.

Wang, Q., Li, F., 2003. On-line monitoring the in-core power distribution by using excore ion-chambers. J. Nucl. Eng. Des. 225, 315–326.

Warsa, S., Wareing, A., Morel, E., McGhee, M., 2004. Krylov subspace iterations for deterministic *k* Eigenvalue calculations. J. Nucl. Sci. Eng. 147, 26–42.

Zinzani, F., Demaziere, C., Sunde, C., 2008. Calculation of the eigenfunctions of the two-group neutron diffusion equation and application to modal decomposition of BWR instabilities. J. Ann. Nucl. Energy 35, 2109–2125.

Liangzhi Cao, born in February 1978, received his PhD in Nuclear Engineering from Xi'an Jiaotong University in 2005. He has been an associate professor in Xi'an Jiaotong University since October 2008, a lecturer in Xi'an Jiaotong University during 2007 to 2008; a Post-doc researcher in the University of Tokyo during 2006 to 2007 and a Post-doc in the Korea Advanced Institute of Science and Technology during 2005 to 2006. Dr. Cao has authored over 40 refereed papers in several journals and conferences. He served as the assistant chairperson of the Technical Program Chair of ICONE18.